Wavelength-swept Tm-doped fiber laser operating in the two-micron wavelength band

M. Tokurakawa,[1,3,*] J. M. O. Daniel,[1] C. S. Chenug,[2] H. Liang,[2] and W. A. Clarkson[1]

[1]*Optoelectronics Research Centre, University of Southampton, Highfield, SO17 1BJ, UK*
[2]*School of Science & Technology, Nottingham Trent University, Nottingham NG11 8NS, UK*
[3]*Present address: Institute of Laser Science, University for Electro-Communications, 1-5-1 Cho-fugaoka, Cho-fu, 182-8585, Tokyo, Japan*
**tokura@ils.uec.ac.jp*

Abstract: A wavelength-swept thulium-doped silica fiber laser using an intracavity rotating slotted-disk wavelength scanning filter in combination with an intracavity solid etalon for passive control of temporal and spectral profiles is reported. The laser yielded a wavelength swept output in a step-wise fashion with each laser pulse separated from the previous pulse by a frequency interval equal to the free-spectral-range of the etalon and with an instantaneous linewidth of <0.05 nm. Scanning ranges from 1905 nm to 2049 nm for a cladding-pumping laser configuration, and from 1768 nm to 1956 nm for a core-pumping laser configuration were achieved at average output powers up to ~1 W.

OCIS codes: (140.3600) Lasers, tunable; (140.3510) Lasers, fiber.

References and links

1. S. R. Chinn, E. A. Swanson, and J. G. Fujimoto, "Optical coherence tomography using a frequency-tunable optical source," Opt. Lett. **22**(5), 340–342 (1997).
2. H. Liang, R. Lange, B. Peric, and M. Spring, "Optimum spectral window for imaging of art with optical coherence tomography," Appl. Phys. B **111**(4), 589–602 (2013).
3. V. M. Kodach, D. J. Faber, and T. G. van Leeuwen, "Wavelength swept Ti:sapphire laser," Opt. Commun. **281**(19), 4975–4978 (2008).
4. V. J. Srinivasan, R. Huber, I. Gorczynska, J. G. Fujimoto, J. Y. Jiang, P. Reisen, and A. E. Cable, "High-speed, high-resolution optical coherence tomography retinal imaging with a frequency-swept laser at 850 nm," Opt. Lett. **32**(4), 361–363 (2007).
5. F. D. Nielsen, L. Thrane, K. Hsu, A. Bjarklev, and P. E. Andersen, "Semiconductor optical amplifier based swept wavelength source at 1060 nm using a scanning Fabry–Perot filter and an YDFA-based booster amplifier," Opt. Commun. **271**(1), 197–202 (2007).
6. S. H. Yun, C. Boudoux, G. J. Tearney, and B. E. Bouma, "High-speed wavelength-swept semiconductor laser with a polygon-scanner-based wavelength filter," Opt. Lett. **28**(20), 1981–1983 (2003).
7. S. H. Yun, D. J. Richardson, D. O. Culverhouse, and B. Y. Kim, "Wavelength-swept fiber laser with frequency shifted feedback and resonantly swept intra-cavity acoustooptic tunable filter," IEEE J. Sel. Top. Quantum Electron. **3**(4), 1087–1096 (1997).
8. W. Y. Oh, B. J. Vakoc, M. Shishkov, G. J. Tearney, and B. E. Bouma, ">400 kHz repetition rate wavelength-swept laser and application to high-speed optical frequency domain imaging," Opt. Lett. **35**(17), 2919–2921 (2010).
9. J. Geng, Q. Wang, J. Wang, S. Jiang, and K. Hsu, "All-fiber wavelength-swept laser near 2 μm," Opt. Lett. **36**(19), 3771–3773 (2011).
10. D. Y. Shen, J. K. Sahu, and W. A. Clarkson, "High-power widely tunable Tm:fibre lasers pumped by an Er,Yb co-doped fibre laser at 1.6 mum," Opt. Express **14**(13), 6084–6090 (2006).
11. T. H. Tsai, C. Zhou, D. C. Adler, and J. G. Fujimoto, "Frequency comb swept lasers," Opt. Express **17**(23), 21257–21270 (2009).
12. M. Jeon, U. Jung, J. Song, J. Kim, J.-H. Oh, J.-S. Eom, C.-S. Kim, and Y.-H. Park, "Frequency swept laser at 1300 nm using a wavelength scanning filter based on a rotating slit disk," Journal of the Optical Society of Korea **13**(3), 330–334 (2009).
13. R. Huber, M. Wojtkowski, and J. G. Fujimoto, "Fourier Domain Mode Locking (FDML): A new laser operating regime and applications for optical coherence tomography," Opt. Express **14**(8), 3225–3237 (2006).
14. R. Scheps and J. F. Myers, "Performance of a diode-pumped laser repetitively Q-switched with a mechanical shutter," Appl. Opt. **33**(6), 969–978 (1994).
15. S. Moon and D. Y. Kim, "Normalization detection scheme for high-speed optical frequency-domain imaging and reflectometry," Opt. Express **15**(23), 15129–15146 (2007).

#213458 - $15.00 USD Received 4 Jun 2014; revised 21 Jul 2014; accepted 28 Jul 2014; published 12 Aug 2014

1. Introduction

Wavelength-swept lasers (WS-lasers) have important applications in a number of areas, including spectroscopic characterization of materials and swept-source optical coherence tomography (SS-OCT) [1]. The use of OCT for non-invasive investigation of paintings to provide the information necessary for effective restoration and to aid conservation is one example of an emerging application where operation in the longer wavelength band around ~2 μm brings the advantage of increased penetration depth due to reduced scattering for typical artists' pigments [2]. SS-OCT does not require a detector array which is an advantage in long wavelength-OCT, where a standard Si CCD camera cannot be used and short-wave infrared-sensitive cameras are expensive. There has been considerable effort aimed at realizing WS-lasers based on different laser gain media for accessing various wavelength bands (*e.g.* ~800 nm with Ti:Al_2O_3 or semiconductor optical amplifiers (SOAs) [3,4], ~1 μm with SOAs and Yb-doped fibers [5], ~1.3 μm with SOAs [6], ~1.5 μm with Er-doped fibers [7]). At the same time, several kinds of wavelength sweeping arrangements (*e.g.* a diffraction grating with a rotating polygon mirror or a galvo scanned mirror [3,4,6], a fiber Fabry-Perot Tunable Filter (FFP-TF) [5], an Acousto-Optic tunable filter (AOTF) [7]) have been investigated. The SOA has emerged as one of the most attractive gain media for WS-lasers due to its relatively broad gain bandwidth, very short lifetime and large emission cross-section allowing high speed broadband WS-laser operation [8]. SOAs operating in the two-micron wavelength band can be achieved through the use of an appropriate quantum well structure, but the performance specifications (e.g. bandwidth, output power) achieved to date are rather limited. Tm-doped silica fiber lasers also provide an efficient way to access the relevant wavelength regime benefiting from a very wide emission band that extends from ~1700 nm to ~2100 nm. Recently, a wavelength-swept Tm fiber laser based on a FFP-TF with a scanning range from 1840 nm to 2040 nm and a maximum output power at the center of the tuning range of ~80 mW was reported [9].

In this paper, we describe a wavelength-swept Tm-doped silica fiber laser operating in the two-micron band that employs a novel external feedback cavity design comprising a diffraction grating, a rotating slotted disk and an intracavity tilted etalon. The external cavity provides time varying wavelength-dependent feedback with passive control of spectral and temporal profiles, yielding a wavelength scan that occurs in a step-wise fashion with each laser pulse separated in frequency from the previous pulse by a frequency interval equal to the free-spectral-range (FSR) of the etalon. The WS-laser was operated in both cladding-pumped and core-pumped configurations yielding scanning ranges of 1905 – 2049 nm and 1768 - 1956 nm, respectively. A maximum output power up to 1.05 W for the scan repetition rates of 400 Hz was obtained for the cladding-pumped WS-laser.

2. Swept source design

The laser resonator design used in our experiment is illustrated in Fig. 1. The accessible emission band of a Tm fiber laser strongly depends on the details of the laser design due to the combination of varying quasi-three-level character as a function of wavelength and gain saturation due to short-wavelength amplified spontaneous emission [10]. Here, we have exploited two different configurations to access different emission bands of Tm-doped fibers.

The first was a cladding-pumped configuration (see Fig. 1(a)) which employed a double-clad Tm-doped silica fiber (fabricated in-house) with an 11-μm diameter core and a 125-μm diameter D-shaped inner-cladding surrounded by a low refractive index polymer coating. The Tm doping level was approximately 2wt.%. Pump light was provided by two 6-W fiber-coupled laser diodes at 793 nm, which were launched into the active Tm fiber via a tapered-fiber-bundle pump coupler with two pump ports and a passive single-mode feed-through fiber. The latter was spliced to the Tm fiber and a fiber length of 3 m was selected for efficient absorption of the launched pump light. A section of passive single-mode fiber was also spliced to the opposite (output) end of the active fiber. Feedback for lasing was provided by a perpendicularly-cleaved fiber facet at the output end of the fiber and by an external

#213458 - $15.00 USD Received 4 Jun 2014; revised 21 Jul 2014; accepted 28 Jul 2014; published 12 Aug 2014

feedback cavity at the opposite end. An angled fiber facet at the fiber end adjacent to the external cavity was used to suppress broadband feedback and hence parasitic lasing between the fiber ends. The external cavity comprised a diffraction grating (600 lines/mm), a rotating slotted-disk and a high reflectivity plane feedback mirror for providing the required time-varying wavelength scanning filter. Two parabolic mirrors were also employed in the external cavity. The first one (90° off-axis with a focusing length of 25.4 mm) was used for collimating the fiber output and the second one (15° off-axis with a focusing length of 304.8 mm) was used for imaging onto the feedback mirror. These were chosen in preference to standard lenses to reduce chromatic and spherical aberration to achieve a broad scanning range in the 2μm band, where commercial achromatic lens are not currently available. The rotating slotted-disk was manufactured in-house and had a diameter and thickness of 152 mm and 0.5 mm, respectively. It had 10 radially-orientated slots, each with a slit-width of 120 μm (see inset of Fig. 1). The width of the slit was selected to match the focused beam diameter of the intracavity laser beam on the final feedback mirror at a particular wavelength. The distance between the feedback mirror and the disk was ~1 mm, and hence much shorter than the Rayleigh range of the focused beam. The resolution of this wavelength scanning filter is estimated to be ~0.6 nm around 2 μm. During the experiments, a solid tilted etalon was also inserted in the collimated section of the beam between the first parabolic mirror and the grating. The purpose of the etalon was to provide passive control of the spectral and temporal profiles of the WS-laser during the wavelength scan. With the etalon present in the external cavity, feedback for lasing is provided only when the wavelength selected by the rotating slotted-disk coincides with transmission peak for the etalon. The net result is that the WS-laser output is a series of equally spaced pulses, each one separated in frequency from the previous pulse by a frequency interval equal to one FSR of the etalon. This avoids the scenario where, in the absence of the etalon, the wavelength-swept output is a series of randomly timed pulses with wide and unequal wavelength separations. The use of an etalon in this manner is similar to the frequency comb swept laser reported by T. Tsai *et al.* in [11].

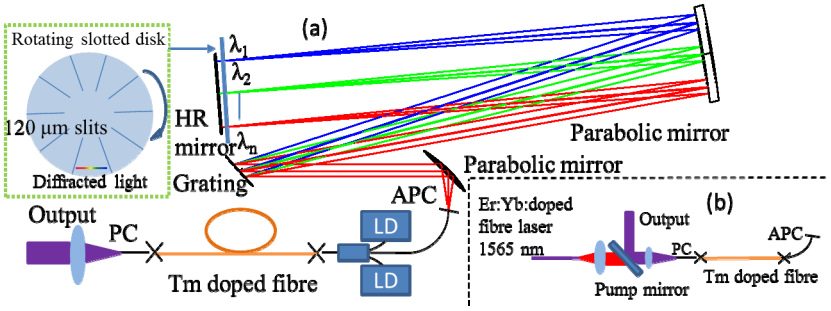

Fig. 1. (a) Schematic diagram of the cladding-pumped Tm-doped fiber WS-laser based on a rotating slotted-disk. The inset at the left side shows the front view of the rotating slotted-disk. (b) Schematic diagram of the core-pumped WS-laser. The angled fiber end (APC) was connected to a similar external cavity unit as used in the cladding-pumped configuration. The cross marks are splicing points. LD is laser diode.

The second laser configuration employed a core-pumped Tm fiber (see Fig. 1(b)) to yield laser output towards the short wavelength end of the Tm:silica emission band. An in-house fabricated Tm-doped silica fiber with a 10-μm diameter core and a relatively low Tm doping level of 0.2 wt.% was employed. In this case, pump light was provided by a commercial Er,Yb fiber laser at 1565 nm that was launched into the core of a passive single-mode fiber spliced to the output end of a 0.9 m length of active fiber. A dichroic mirror was used to separate the laser output from the pump beam. The use of a core-pumped fiber configuration yields a much higher population inversion density than in a cladding-pumped configuration and hence provides the necessary gain at the short wavelength end of the emission band to access lasing in this region. The other components used in the resonator (e.g. external cavity) were the same as those employed in the cladding-pumped WS-laser.

#213458 - $15.00 USD Received 4 Jun 2014; revised 21 Jul 2014; accepted 28 Jul 2014; published 12 Aug 2014

3. Results and discussion

First, the cladding-pumped WS-laser operation was tested without the etalon. The scanning frequency was 200 Hz. Measured spectral and temporal profiles are shown in Fig. 2. The measured temporal profile shows pulsing behavior with poor amplitude and timing stability. This impacts directly on the spectral profile with the result that the evolution of the lasing wavelength with time during a scan is not smooth (i.e. the wavelength spacing between successive pulses can change significantly depending on the time interval as can the spectral power density). This behavior is quite different from that routinely observed in WS-lasers based on SOA gain media [8, 12], and can be attributed to the long upper-state lifetime and low emission cross-section for rare-earth doped gain media leading to a long build-up time for laser emission. The use of Fourier domain mode-locking could suppress the instability by virtue of the self-seeding effect [13], but the requirement for a long length of fiber would make this extremely difficult to implement in the two-micron band due to the higher propagation loss.

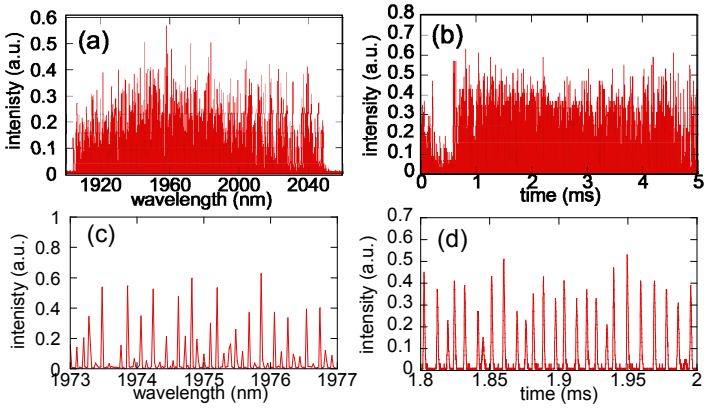

Fig. 2. Output spectral and temporal profiles of the WS-laser for the cladding-pumped configuration without an etalon. (a) Whole spectrum and (b) temporal profiles for a sweep. (c) Local spectral and (d) temporal profiles.

To remedy this problem we employed a tilted intracavity fused silica etalon with an FSR of ~34.8 GHz to provide a passive means for controlling the pulsing behavior rather than attempting to suppress it. Due to the insertion loss of the etalon, output power of the WS-laser decreased by ~20%. The measured output spectral and temporal profiles of the WS-laser with the etalon are shown in Fig. 3. The measured spectrum showed comb-like shape with regularly spaced pulses separated by a frequency interval equal to the FSR of the etalon. The wavelength positions of the peaks in the spectrum could be adjusted within the FSR by simply changing the angle of the etalon (see Fig. 3(c)). The temporal profile also showed regular pulsing behavior with a constant time interval between pulses corresponding to the FSR of the etalon divided by the scanning speed of the tunable filter. The wavelength scanning range achievable with this set-up was from 1905 nm to 2049 nm, and the average output power was 510 mW for 6 W of pump power. The measured linewidth for each pulse was <0.05 nm (limited by resolution of our optical spectral analyzer) and the pulse duration was ~500 ns.

To further investigate the relationship between the measured spectral and temporal profiles of the WS-laser (Fig. 3), we isolated each spectral component using a monochromator and measured its temporal behavior with an oscilloscope. This measurement confirmed that each pulse corresponds to a single wavelength peak in the spectral profile and there was no evidence of simultaneous multi-wavelength operation during successive sweeps. In other words, for successive laser pulses during a wavelength sweep the lasing wavelength increments by one FSR of the etalon. Hence, the temporal profile also shows the spectral

#213458 - $15.00 USD Received 4 Jun 2014; revised 21 Jul 2014; accepted 28 Jul 2014; published 12 Aug 2014

profile (power spectrum) of the WS-laser for a single shot. The optical spectrum analyzer (OSA) used for direct measurement of the output spectrum was not synchronized to the WS-laser, hence sampling errors may give rise to artificial noise in the measured power spectrum.

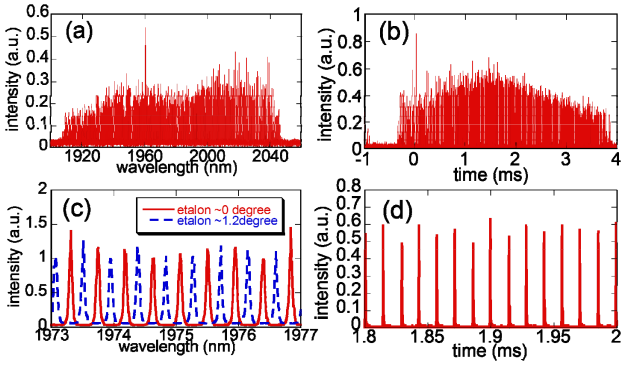

Fig. 3. Output spectral and temporal profiles of the WS-laser for the cladding-pumped configuration with the etalon. (a) Whole spectrum and (b) temporal profiles for a sweep. (c) Local spectral and (d) temporal profiles.

WS-laser operation was also investigated under core-pumping condition at a scanning frequency of 200 Hz with the intracavity etalon. The measured spectral and temporal profiles (shown in Fig. 4) show similar comb-like behavior to the cladding-pumped WS-laser, but with a broader scanning range from 1768 nm to 1956 nm. The maximum average output power was 330 mW for pump power of 2.4 W.

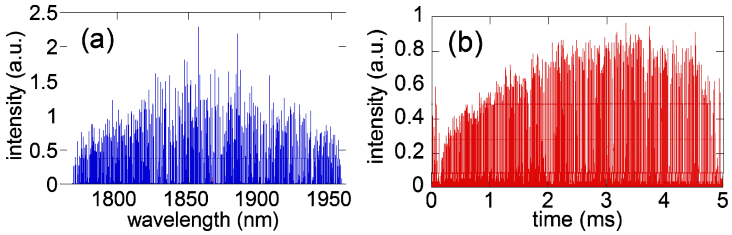

Fig. 4. (a) Output spectral and (b) temporal profiles of the WS-laser for the core-pumped configuration with the etalon.

The cladding-pumped WS-laser was also operated at a higher scanning frequency of 400 Hz with an etalon of FSR, 52.2 GHz. Once again, step-wise incrementing of the lasing wavelength for successive laser pulses (controlled by the intracavity etalon) was observed (Fig. 5). The average output power increased to 1.05 W for a pump power of 7.5 W. At the shoulders of the sweep, some irregular pulsing was observed with the wavelength spacing between adjacent pulses increasing by a factor-of-two (see Fig. 5(b)). This behavior can be attributed to lower gain at the extreme ends of the tuning curve and can be eliminated by increasing the pump power. However, this was found to lead to the appearance of additional sub-pulses around the middle part of the peak due to the higher gain yielding a lasing build-up time that is shorter than the opening time of the rotating slotted disk (~7 μs for 400 Hz). This behavior is analogous to that observed in Q-switched lasers when the build-up time is short compared with the Q-switch opening time [14]. The peak intensity at each wavelength in the sweep showed only a small fluctuation for successive sweeps. The measured standard deviation (STD) of peak intensity as a function of wavelength (shown in Fig. 6) was typically in the range 3 - 5% over a bandwidth of ~120 nm. Outside this band, the fluctuations become larger for the reasons explained above and possibly exacerbated by mechanical tolerance in the slotted disk. These fluctuations are not expected to be an issue for most applications [15]. The maximum scanning frequency was limited by vibration of the rotating slotted disk. The

#213458 - $15.00 USD Received 4 Jun 2014; revised 21 Jul 2014; accepted 28 Jul 2014; published 12 Aug 2014

use of an improved mechanical arrangement for mounting the slotted disk and electric motor should allow the scanning frequency to be increased to >1 kHz.

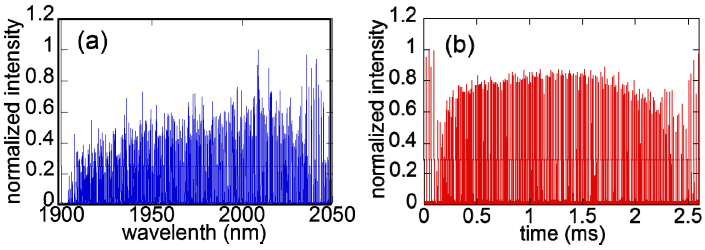

Fig. 5. (a) Output spectral and (b) temporal profiles of the WS-laser for the cladding-pumped configuration with the etalon at 400 Hz scanning frequency.

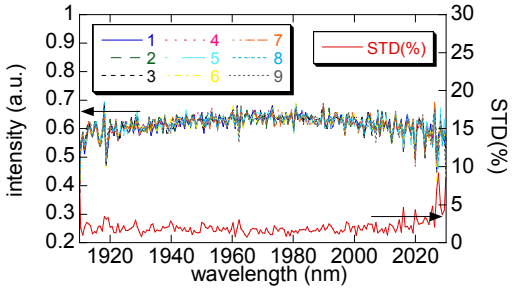

Fig. 6. Variation of the peak intensities at each wavelength for successive sweeps and resulting standard deviations. Data for 9 sweeps are shown.

4. Conclusion

In summary, we have demonstrated a novel wavelength-swept Tm-doped silica fiber laser operating in the two-micron wavelength band and employing an external feedback cavity with a diffraction grating and a rotating slotted-disk to provide time varying wavelength-dependent feedback. Passive control of the spectral and temporal profiles to eliminate spurious laser pulses was achieved with the aid of an intracavity tilted etalon. This allows wavelength sweeping in a step-wise fashion with each laser pulse separated from the previous pulse by a frequency interval equal to the free-spectral-range of the etalon. Scanning ranges from 1905 nm to 2049 nm (for cladding-pumping) and from 1768 nm to 1956 nm (for core-pumping) were obtained with excellent spectral power stability. Average power levels up to 1.05 W and scanning frequencies up to 400 Hz were achieved, but there is scope for increasing both through optimization of the cavity design to flatten the gain spectrum and with the availability of higher pump power. This approach for generating wavelength-swept output in the two-micron band should benefit range of applications in spectroscopy, sensing and optical coherence tomography.

Acknowledgments

Funding from UK Art and Humanities Research Council (AHRC) and Engineering and Physical Sciences Research Council (EPSRC) Science & Heritage Program (Interdisciplinary Research Grant AH/H032665/1) is gratefully acknowledged.